Original Article
Comparison of autotaxin expression level and ultrasonic characteristics in patients with ovarian epithelial carcinoma and ovarian epithelial benign tumor

Zhiling Zhang, Ling Xu, Zheng Hu, Li Li, Chao Xu, Jun Xu

Department of Obstetrics and Gynecology, Central Hospital of Minhang District, Shanghai 201100, China

Abstract: The purpose of this study was to compare autotaxin expression level and ultrasonic characteristics in patients with ovarian epithelial carcinoma and ovarian epithelial benign tumor. Twenty-six cases of ovarian epithelial benign tumor, 38 cases of epithelial ovarian carcinoma, and 18 cases of normal ovarian tissues were examined. The expression of ATX mRNA and protein were analyzed by western blot and immunohistochemistry. The results showed that ATX protein and mRNA expression was detected in three types of tissues. ATX mRNA expression was higher in ovarian epithelial carcinoma than that in normal ovarian tissues and ovarian epithelial benign tumor (P<0.05). Western blot showed clear ladders of ATX protein at around 55 kDa in ovrian carcinoma tissues. Immunohistochemistry results also demonstrated that ATX protein expression in ovarian epithelial carcinoma was higher than that in ovarian epithelial benign tumor. In ovarian epithelial benign tumor groups, majority appearance of tumor location showed middle to low (84.6%), uniformity (80.8%) and sharpness of boundary of enhanced lesions (88.5%), while minority of tumor showed middle to low (18.4%), uniformity (23.7%) and sharpness of boundary of enhanced lesions in ovarian epithelial carcinoma groups. In conclusion, the differences in expression of ATX and ultrasonic characteristics in ovarian epithelial carcinoma and ovarian epithelial benign tumor can be used to estimate early diagnosis, therapeutic regimen and prognosis in ovarian neoplasm.

Keywords: Cancer, autotaxin (ATX), ultrasound, ovarian epithelial carcinoma

Introduction

Ovarian cancer is the most deadly type of cancer worldwide in women [1, 2]. The Patients with ovarian cancer have high mortality and poor prognosis. This is obviously related to the occult incidence of ovarian cancer, the difficulty of early diagnosis, and the limitations of existing treatment measures [3]. It is urgent to find simple, rapid, and highly sensitive methods for ovarian cancer diagnosis.

Autotaxin (ATX) is an ecto-nucleotide pyrophosphatase/phosphodiesterase-2 enzyme [5]. It played an important role in hydrolyzing extracellular lysophospholipids into lysophosphatidic acid (LPA) [6, 7]. LPA enhances lymphocyte invasion and cytokine production, as well as increasing VEGF production to stimulate angiogenesis, which is required for tumor growth and metastasis and decreased response to chemotherapy. Increased expressions of ATX and LPA1-3 receptors were related to the occur-

rence and development of cancer in mice or women. The results suggested that the ATX-LPA signal pathway was physiologically correlated [8, 9]. Imbalance of ATX-LPA signaling pathway is correlated with neuropathic pain, fibrosis, and cancers and rheumatoid arthritis [10, 11]. There is growing evidence that ATX played a benefit for clinical application in cancer [12].

At present, ultrasound has been extensively used in clinic and is still an important tool for diagnosing cancers. There are several disadvantages that exist, for example, it can easily miss diagnosis in cavity organs, the results can be easily interfered by gases or technological level of doctor [13-15]. So it is urgent to find the new clinical index to diagnose cancers. Although ATX is important, the role of ATX in cancer diagnosis and therapy remained to be studied.

The purpose of this study was to compare autotaxin expression level and ultrasonic characteristics in patients with ovarian epithelial carcinoma and ovarian epithelial benign tumor.

Table 1. General clinical data [n (%)]

Categories	Normal ovarian group (n=18)	Ovarian epithelial benign tumor group (n=26)	Ovarian epitheiial carcinoma group (n=38)	P value
Age	53.75±1.26	53.48±1.33	53.95±1.74	>0.05
Body weight (kg/m^2)	23.42±2.05	23.77±2.19	23.86±2.78	>0.05
Place of residence				>0.05
City	10 (55.56)	14 (53.85)	21 (55.26)	
Countryside	8 (44.44)	12 (46.15)	17 (44.74)	
Nationality				>0.05
Han	12 (66.67)	17 (65.38)	25 (65.79)	
National minorities	6 (33.33)	9 (34.62)	13 (34.21)	
Educational history				>0.05
≥ Senior high school	11 (61.11)	16 (61.54)	24 (63.16)	
< Senior high school	7 (38.89)	10 (38.46)	14 (36.84)	

Materials and methods

Materials

SYBR, FBS, L-glutamine and β-mercaptoethanol, minimum essential amino acids, goat anti-mouse IgGs, anti-ATX-4 and anti-GAPDH were all purchased from commercial corporation. The other reagents were commercially available. Real-time color Doppler ultrasonography (Parkson, Italy) was used for contrast-enhanced ultrasonography.

Patients and tissue samples

Tissues were obtained from 64 female patients who underwent initial oophorectomy at the hospital (China) between May 2013 and June 2017. In these patients, 26 suffered from benign ovarian tumor and 38 were diagnosed with ovarian cancer. All patients were not treated with radiation, chemotherapy and immunotherapy. The inclusion criteria were: Subjects could provide the signature to the informed consent form (ICF); female at more than 20 years of age; the histopathological specimens could be submitted to the central pathological labs. Another 18 normal ovarian tissues were taken from female patients who underwent hysteromyomectomy. All fresh tissues removed from operation were preserved in liquid nitrogen after extirpated necrotic areas and then stored at -80°C.

Ultrasound contrast

The ultrasound contrast was made by real-time color Doppler ultrasonography (Parkson, Italy). Frequency of array test was 5-13 MHz, frequency of imaging probe was 4-7 MHz, and mechanism index was 0.08-0.11. Shadowgraph technique was used (SonoVue, Braceo, Italy) [16].

RNA Isolation and real-time PCR

Reported methods were used to extract total RNA from tumor tissues [17]. A cDNA synthesis kit was used to cDNA synthesis. Relative transcript levels of ATX were determined by RT-PCR. Primers for ATX gene (GenBank Accession ID: NC_000008.11) were signed depended on the sequence of cDNA for human ovarian tumor cell. The GAPDH (ID: NM_001289746.1) was also designed.

Primers are as follows: ATX FP 5'-TAAAAC-AGTACGTGAAGGCAGTT-3' and RP 5'-GTGTGCA-TCTTCATGAGTTCTTCT-3'. GAPDH: FP 5'GACACC-CACTCCTCCACCTTT3' and RP 5'TGTTGCTGTA-GCCAAATTCGTT3'.

Western blot

Tissues were disrupted with cold (-10°C) RIPA buffer and BCA kit, and the protein concentration was determined. Total protein was separated and transferred to a preactivated polyvinylidene fluoride membrane. The membranes were blocked using 4% dried skim milk in TBS at 4°C for 1.5 hours and incubated with primary antibodies (diluted 1:3000) at 4°C for 12 hours. Then membranes were washed five times by TBST and compressed with secondary antibodies (diluted 1:5000) at room temperature for 1.5 hours. At last, the membrane was wash extensively and hatched using ECL chemiluminescent kit (Thermo Scientific, USA).
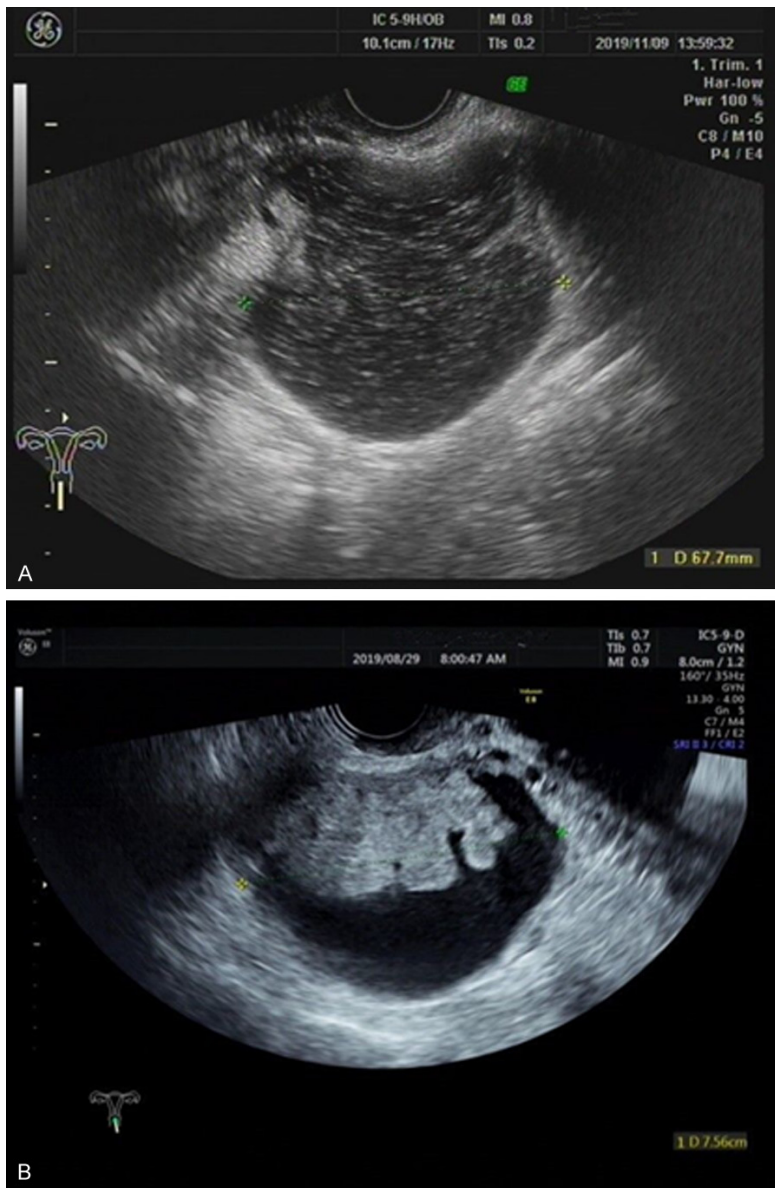
Figure 1. Original figures of ultrasonic of ovarian epithelial benign tumor (A) and ovarian epitheiial carcinoma (B).

Immunofluorescence

All tissues were fixed with 10% unbuffered formalin, followed by paraffin imbedding and section. The expression of ATX was analyzed by immunofluorescence staining with ATX. The 3.5% paraformaldehyde was used to fix. After fixed, PBS was used to wash the cells, and then they were incubated with blocking buffer. The primary antibody was diluted. After incubation with secondary antibodies conjugated with SP for 1.5 hour at 37°C, followed by wash 3 times in PBS, fluorescence microscope was used to obtain pictures [18].

Statistical analysis

Data were analyzed with SPSS 25.0 software (SPSS, Chicago, IL, USA). The enumeration data was expressed in n (%), and chi-square test was performed. The measurement data was represented by mean ± SD. Group comparisons of age, body weight, expression of ATX mRNA and protein were performed using one-way ANOVA. The *p*-values less than 0.05 indicate statistical significance.

Results

Comparison of general information

There was no significant difference among the three groups (normal ovarian group, ovarian epithelial benign tumor group, ovarian epithelial carcinoma group) in the age, body weight, place of residence, nationality, and educational history (P> 0.05) (**Table 1**).

Ultrasonic features displayed complete difference in two tissues

In ovarian epithelial benign tumor group, the majority appearance of tumor location showed middle to low (84.6%), uniformity (80.8%) and sharpness of boundary of enhanced lesions (88.5%), while minority of tumor showed middle to low (18.4%), uniformity (23.7%) and sharpness of boundary of enhanced lesions in ovarian epithelial carcinoma group (13.2%). The difference of the above ultrasonic features between ovarian epithelial carcinoma and ovarian epithelial benign tumor was statistically significant (P<0.05) (**Figure 1** and **Table 2**).

Table 2. Comparison of ultrasonic characteristics

| Group	Enhanced degree				Uniformity				Boundary			
	Middle to low		High		Uniformity		Inhomogeneity		Sharpness		Unsharpness	
	n	%	n	%	n	%	n	%	n	%	n	%
Ovarian epithelial benign tumor group(n=26)	22	84.6	4	15.4	21	80.8	5	19.2	3	11.5	23	88.5
Ovarian epitheiial carcinoma group (n=38)	7	8.4*	31*	81.6*	9	23.7	29	76.3*	33	86.8*	5	13.2*

*, represents a comparison with the ovarian epithelial benign tumor group, P<0.05.
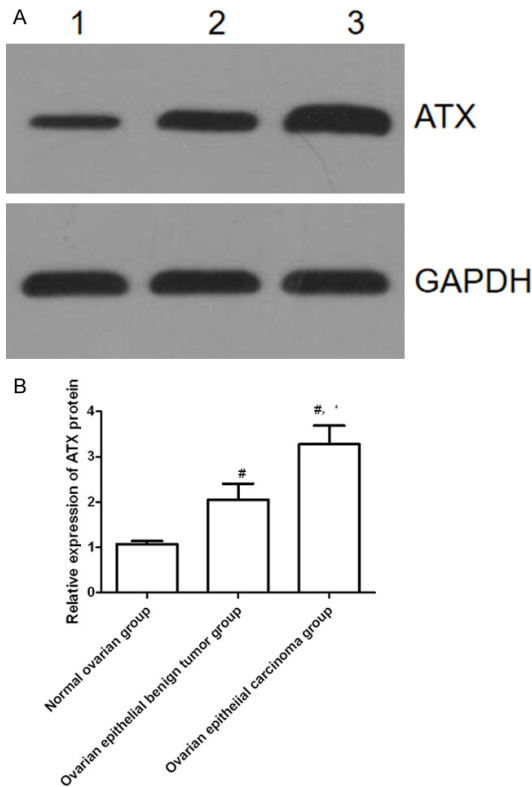
Figure 2. The levels of ATX protein in all groups. A: Detection of proteins. B: Quantitative analysis. The expression levels of ATX protein and GADPH protein were detected by mouse anti-ATX monoclonal antibody or mouse anti-GADPH lysine monoclonal antibody. 1: normal ovarian group (n=18). 2: ovarian epithelial benign tumor group (n=26). 3:ovarian epitheiial carcinoma group (n=38). #, represents a comparison with the normal ovarian group, P<0.05. *, represents a comparison with the ovarian epithelial benign tumor group, P<0.05.

Comparison of expression levels of ATX mRNA in different tissues

The relative expressions of ATX mRNA were normalized in tumor tissues. Amplification efficiency of ATX mRNA and GAPDH mRNA was obtained by standard curve (data not shown). The ATX mRNA was expressed in all groups. The expression levels in ovarian epithelial carcinoma group were nearly 1.91-fold compared with the ovarian epithelial benign tumor group and
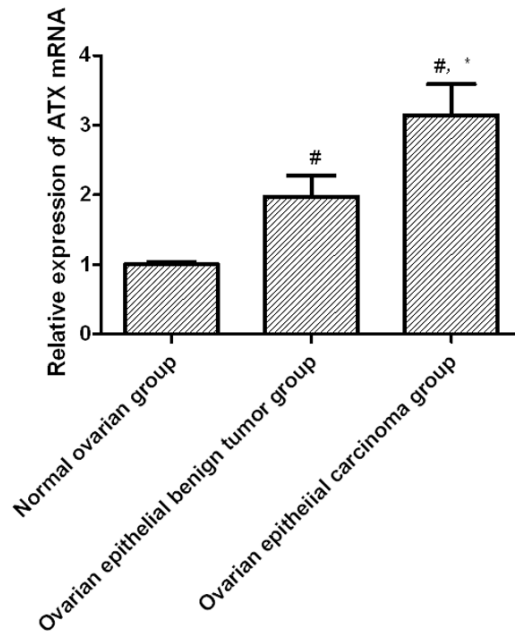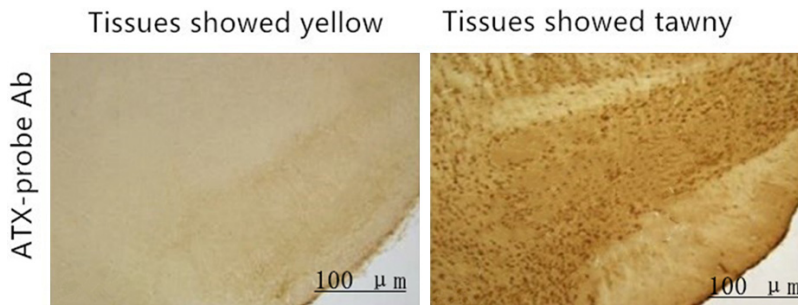

Figure 3. The expression of ATX mRNA in normal ovarian groups, epithelial benign tumor group and ovarian epithelial carcinoma group. #, represents a comparison with the normal ovarian group, P<0.05. *, represents a comparison with the ovarian epithelial benign tumor group, P<0.05.

3.23-fold compared with normal ovarian group (**Figure 2**). The statistical analysis showed significant improvements of ATX mRNA (P<0.01) in ovarian epithelial carcinoma group.

Comparison of expression levels of ATX protein in different tissues using western blot

ATX protein in tumor tissues was analyzed by western blot with GADPH as internal reference [19]. The results showed that ATX protein was expressed in almost all tumor tissues. Results showed that ATX protein in ovarian epithelial carcinoma group was much higher than ovarian epithelial benign tumor group and normal ovarian group (**Figure 3**). The statistical analysis showed significant improvements of ATX protein expression (P<0.01) in ovarian epithelial carcinoma group.

Figure 4. The expression of ATX analyzed by immunostaining analysis.

Table 3. Comparison of expression levels of ATX protein

Group	Color of tissues after SP staining			
	Light yellow		Tawny	
	n	%	n	%
Normal ovarian group (n=18)	14	77.8	4	22.2
Ovarian epithelial benign tumor group (n=26)	14	53.8**	12	46.2**
Ovarian epitheiial carcinoma group (n=38)	16	42.1**,#	22	57.9**,#

**, represents a comparison with the normal ovarian group, P<0.01. #, represents a comparison with the ovarian epithelial benign tumor group, P<0.05.

Comparison of expression levels of ATX protein in different tissues using immunofluorescence

ATX protein in all tissues was also analyzed by immunofluorescence after SP immunohisto-chemical staining (**Figure 4**). ATX protein was observed in majority tissues in ovarian epithe-lial carcinoma group by staining with an anti-ATX tag antibody, so the tissues showed tawny after staining. The ATX protein was unstained in majority of tissues in normal ovarian group and ovarian epithelial benign tumor group and the tissues turned yellow after staining. The tissues in ovarian epithelial carcinoma group almost appeared in yellow (16/38) and tawny (22/38). Most of the tissues in ovarian epithelial benign tumor group were yellow (14/26) or tawny (12/26). Most of the tissues in normal ovarian group were yellow (14/18) or tawny (4/18) (**Table 3**). The results indicated that the ATX protein was significant observed (P<0.01) in ovarian epithelial carcinoma group and ovarian epithelial benign tumor group, but not in normal ovarian group and the levels of ATX protein in ovarian epithelial carcinoma group significantly increased (P<0.05) compared with the ovarian epithelial benign tumor group.

Discussion

It was reported that ovarian cancer showed high mortality for development of resistance to chemotherapy and relapse [20]. ATX, a LPA-producing enzyme, is highly secreted from ovarian (cancer stem cells) CSCs [6, 21]. It is important to analyze the expression levels of ATX in ovarian cancer tissues. A study showed a link between ATX expression, lyso-phosphatidic acid and vascular endothelial growth factor signaling in ovarian cancer cell lines [22]. We analyzed the level of ATX mRNA and protein in ovarian tissues, ovarian epithelial benign tumor tissues and ovarian epithelial carcinoma tissues. The result showed that the expression level of ATX mRNA and protein was markedly higher in ovarian epithelial benign tumor tissues than that in other ovarian tissues. The results suggested that ATX may become an index to diagnose metastatic ovarian cancer. The conclusion of this study was basically consistent with the previous research report that ATX could affect tumor progression in ovarian cancer cells [23]. ATX over-expression in ovarian cancer cells may be associated with aberrant LPA production. However, one study noted that, compared with healthy subjects, serum ATX antigen levels were not increased in ovarian cancer patients, and serum ATX may not be useful as a biomarker for ovarian cancer [24].

Ultrasound examination has the advantages of low cost, simple operation and high repeatability. Compared with histopathological examination, ultrasound examination is non-radiating and convenient [25]. So it is widely used in clinic. The results of this study show that the main ultrasound features of ovarian cancer were the appearances low (84.6%), uniformity (80.8%) and sharpness of boundary of enhanced lesions (88.5%). The minority of tumor showed middle to low (18.4%), uniformity (23.7%) and sharpness of boundary of enhanced lesions (13.2%) in ovarian epithelial carcinoma groups. Two groups of patients compared showed statistically significant difference. This may have connections with the growth pattern of malig-

nant neoplasms. The new vessels of malignant neoplasms were thick and unevenly distributed and resulted in a disordered network. The vessels of focal central areas were smaller. These features may cause the lesion locations low, uniformity and sharpness of boundary. Alcázar et al found that some differences exist between type I and type II epithelial ovarian cancer in clinical and ultrasound manifestations [26]. We believe above research results could provide some clues to clinicians faced with the difficulty in diagnosis of ovarian cancer. The shortcomings of this study lies in the small sample size, which needs further prospective study in clinical application to verify the conclusion of our research.

In conclusion, it can be seen the difference of expression of ATX and ultrasonic characteristics between ovarian epithelial carcinoma and ovarian epithelial benign tumor. This study provides an idea to use ultrasound features as well as ATX expression to diagnosing malignant tumor. The study may provide a method for earlier and more accurate to find malignant tumor and take action more quickly to kill the cancer.

Disclosure of conflict of interest

None.

Address correspondence to: Jun Xu, Department of Obstetrics and Gynecology, Central Hospital of Minhang District, No. 170, Xinsong Road, Minhang District, Shanghai 201100, China. Tel: +86-189-18169258; E-mail: xpmzh0@163.com

References

[1] Biskup K, Braicu EI, Sehouli J, Tauber R and Blanchard V. The ascites N-glycome of epithelial ovarian cancer patients. J Proteomics 2017; 157: 33-39.

[2] Liu SC, Lin H, Huang CC, Chang Chien CC, Tsai CC, Ou YC, Fu HC, Liu JM and Ma YY. Prognostic role of excision repair cross complementing-1 and topoisomerase-1 expression in epithelial ovarian cancer. Taiwan J Obstet Gynecol 2016; 55: 213-219.

[3] Blyuss O, Burnell M, Ryan A, Gentry-Maharaj A, Mariño IP, Kalsi J, Manchanda R, Timms JF, Parmar M, Skates SJ, Jacobs, Zaikin A and Menon U. Comparison of longitudinal CA125 algorithms as a first-Line screen for ovarian cancer in the general population. Clin Cancer Res 2018; 24: 4726-4733.

[4] Schmeler KM, Sun CC, Bodurka DC, Deavers MT, Malpica A, Coleman RL, Ramirez PT and Gershenson DM. Neoadjuvant chemotherapy for low-grade serous carcinoma of the ovary or peritoneum. Gynecol Oncol 2008; 108: 510-514.

[5] Fang YN, Huang ZL, Li H, Tan WB, Zhang QG, Wang L and Wu JL. LINC01116 promotes the progression of epithelial ovarian cancer via regulating cell apoptosis. Eur Rev Med Pharmacol Sci 2018; 22: 5127-5133.

[6] Meng G, Tang X, Yang Z, Benesch MGK, Marshall A, Murray D, Hemmings DG, Wuest F, McMullen TPW and Brindley DN. Implications for breast cancer treatment from increased autotaxin production in adipose tissue after radiotherapy. FASEB J 2017; 31: 4064-4077.

[7] Siess W and Tigyi G. Thrombogenic and atherogenic activities of lysophosphatidic acid. J Cell Biochem 2004; 92: 1086-1094.

[8] Lin YC, Chen CC and Chen WM. LPA1/3 signaling mediates tumor lymphangiogenesis through promoting CRT expression in prostate cancer. Biochim Biophys Acta 2018; 30170-30177.

[9] Ninou I, Magkrioti C and Aidinis V. Autotaxin in pathophysiology and pulmonary fibrosis. Front Med (Lausanne) 2018; 5: 180.

[10] Macias RIR, Matilla S, Lozano E, Estiú MC, Elferink RPO and Marin JJG. Role of the placenta in serum autotaxin elevation during maternal cholestasis. Am J Physiol Gastrointest Liver Physiol 2018; 315: G399-G407.

[11] Masago K, Kihara Y, Yanagida K, Hamano F, Nakagawa S, Niwa M and Shimizu T. Lysophosphatidic acid receptor, LPA6, regulates endothelial blood-brain barrier function: Implication for hepatic encephalopathy. Biochem Biophys Res Commun 2018; 501: 1048-1054.

[12] Magkrioti C, Oikonomou N, Kaffe E, Mouratis MA, Xylourgidis N, Barbayianni I, Megadoukas P, Harokopos V, Valavanis C, Chun J, Kosma A, Stathopoulos GT, Bouros E, Bouros D, Syrigos K and Aidinis V. The autotaxin-lysophosphatidic acid axis promotes lung carcinogenesis. Cancer Res 2018; 78: 3634-3644.

[13] Nie M, Qin Y, Zhu J, Li Y and Wang Z. Correlation between ultrasonic features and expression levels of C-erbB-2, VEGF and nm23 in breast cancer. Oncol Lett 2018; 16: 1701-1707.

[14] Nguyen LT, Kocur GK and Saenger EH. Defect mapping in pipes by ultrasonic wavefield cross-correlation: a synthetic verification. Ultrasonics 2018; 90: 153-165.

[15] Rentala VK, Mylavarapu P and Gautam JP. Issues in estimating probability of detection of NDT techniques-A model assisted approach. Ultrasonics 2018; 87: 59-70.

[16] Chancellor MB, Liu JB, Rivas DA, Karasick S, Bagley DH and Goldberg BB. Intraoperative

endo-luminal ultrasound evaluation of urethral diverticula. J Urol 1995; 153: 72-75.

[17] Dundar E, Sonmez GD and Unver T. Isolation, molecular characterization and functional analysis of OeMT2, an olive metallothionein with a bioremediation potential. Mol Genet Genomics 2015; 290: 187-199.

[18] Kim MJ, Park M, Kim DW, Shin MJ, Son O, Jo HS, Yeo HJ, Cho SB, Park JH, Lee CH, Kim DS, Kwon OS, Kim J, Han KH, Park J, Eum WS and Choi SY. Transduced PEP-1-PON1 proteins regulate microglial activation and dopaminergic neuronal death in a Parkinson's disease model. Biomaterials 2015; 64: 45-56.

[19] Trung Cao T, Tsai MA, Yang CD, Wang PC, Kuo TY, Gabriel Chen HC and Chen SC. Vaccine efficacy of glyceraldehyde-3-phosphate dehydrogenase (GAPDH) from Edwardsiella ictaluri against E. tarda in tilapia. J Gen Appl Microbiol 2014; 60: 241-250.

[20] Haga A, Hashimoto K, Tanaka N, Nakamura KT and Deyashiki Y. Scalable purification and characterization of the extracellular domain of human autotaxin from prokaryotic cells. Protein Expr Purif 2008; 59: 9-17.

[21] Seo EJ, Kwon YW, Jang IH, Kim DK, Lee SI, Choi EJ, Kim KH, Suh DS, Lee JH, Choi KU, Lee JW, Mok HJ, Kim KP, Matsumoto H, Aoki J and Kim JH. Autotaxin regulates maintenance of ovarian cancer stem cells through lysophosphatidic acid-mediated autocrine mechanism. Stem Cells 2016; 34: 551-564.

[22] Malgorzata MP, Michael LP, Russell WB, Mary LS and David DR. Positive feedback between vascular endothelial growth factor-A and autotaxin in ovarian cancer cells. Mol Cancer Res 2008; 6: 352-363.

[23] Seo EJ, Kwon YW, Jang IH, Kim DK, Lee SI, Choi EJ, Kim KH, Suh DS, Lee JH, Choi KU, Lee JW, Mok HJ, Kim KP, Matsumoto H, Aoki J and Kim JH. Autotaxin regulates maintenance of ovarian cancer stem cells through lysophosphatidic acid-mediated autocrine mechanism. Stem Cells 2016; 34: 551-564.

[24] Nakamura K, Igarashi K, Ohkawa R, Yokota H, Masuda A, Nakagawa S, Yano T, Ikeda H, Aoki J and Yatomi Y. Serum autotaxin is not a useful biomarker for ovarian cancer. Lipids 2012; 47: 927-930.

[25] Regelsberger J, Delling G, Helmke K, Tsokos M, Kammler G, Kränzlein H and Westphal M. Ultrasound in the diagnosis of craniosynostosis. J Craniofac Surg 2006; 17: 623-625.

[26] Alcázar JL, Utrilla-Layna J, Mínguez JÁ and Jurado M. Clinical and ultrasound features of type I and type II epithelial ovarian cancer. Int J Gynecol Cancer 2013; 23: 680-684.